ACS OMEGA

Open Access

http://pubs.acs.org/journal/acsodf

Article

Temperature Control Minimizes Wax-Derived Alkane Carryover in Hydrocarbon Cannabis Extraction

Manuel E. Sosa, Twinkle R. Paryani, Randy J. Reed, Alex W. Siegel, Qianxiang Ai, Eugene Lee, Daniel L. Radford, Thomas J. Martin, Kevin A. Koby, and Iain W. H. Oswald*

Cite This: https://doi.org/10.1021/acsomega.5c13451

Read Online

ACCESS | Metrics & More | Article Recommendations | Supporting Information

ABSTRACT: Cannabis produces a diverse array of nonpolar metabolites, including cannabinoids and terpenes, making nonpolar hydrocarbon solvents well-suited for extracting inhalable concentrates. In practice, these extracts also contain a poorly characterized nonpolar fraction colloquially termed "fats and waxes," which can be removed by winterization. To clarify the composition and process dependence of this fraction, we examined *n*-butane extractions of two cannabis varieties (GMO and Oreoz) across the industrially relevant temperature range of −46 °C to −9 °C. Using GC×GC−TOF−MS/FID, we identified long-chain *n*-alkanes (C_{22}−C_{31}), consistent with epicuticular wax constituents, as major components whose abundance increases systematically with extraction temperature, while total cannabinoids and quantified volatile aroma compounds remain relatively constant over the same range. Viscosity measurements show only modest changes with wax loading, indicating limited impact on bulk rheology at the concentrations studied. Aerosol capture experiments demonstrate that these *n*-alkanes transfer efficiently into the mainstream aerosol and that aerosol wax levels track their concentrations in the starting high-terpene extract with an approximately linear relationship. Lowering the extraction temperature reduces both wax content in the oil and the corresponding wax dose in the aerosol, with up to ≈3-fold reductions depending on cultivar. These results establish extraction temperature as a practical control point for minimizing epicuticular wax coextraction in hydrocarbon-derived cannabis concentrates, demonstrating that lower temperatures selectively reduce long-chain *n*-alkane content while preserving cannabinoid potency and native-like aroma profiles. The efficient transfer of these alkanes into mainstream aerosol further indicates that extraction conditions directly influence consumer inhalation exposure to wax-derived constituents.

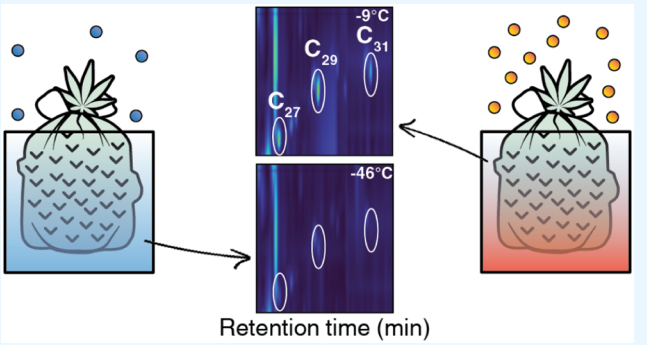

INTRODUCTION

The rapid legalization of cannabis across North America and Europe over the past decade has driven substantial growth in both medical and recreational markets.[1] Consumer demand has expanded beyond dried flower to include highly concentrated formulations, particularly vaporization-based products ("vapes"), which offer consistent dosing, discretion, and rapid onset.[2] Vaping has become a dominant inhalation modality owing to its convenience, potency, and perceived health benefits relative to combustion.[3] Concurrent with the industry's transition from an illicit to a regulated market, product development and extraction technologies have become central to differentiating quality, consistency, and sensory performance. Cannabis contains hundreds of chemically diverse constituents spanning a wide range of volatilities, polarities, and thermal stabilities, each of which may respond differently to drying, storage, and extraction conditions. Despite the commercial importance of these processes, systematic scientific investigations into how processing variables affect cannabis chemistry remain limited.

Cannabis sativa L. produces more than 100 identified cannabinoids and hundreds of volatile organic compounds (VOCs), including monoterpenes, sesquiterpenes, their oxygenated derivatives, and various nonterpenoid flavorants.[4−6] Collectively, these phytochemicals define the plant's chemotype and sensory properties.[5,6] Commercial extracts can be broadly categorized into three chemical fractions: (i) major cannabinoids, such as Δ^9-tetrahydrocannabinol (THC), cannabidiol (CBD), and their acidic precursors THCA and CBDA; (ii) volatile aroma constituents responsible for cultivar-specific flavors and aromas; and (iii) a minor but variable ancillary fraction comprising waxes, pigments, and other nonvolatile phytochemicals. Whereas cannabinoids and

Received: December 23, 2025
Revised: June 3, 2026
Accepted: June 15, 2026

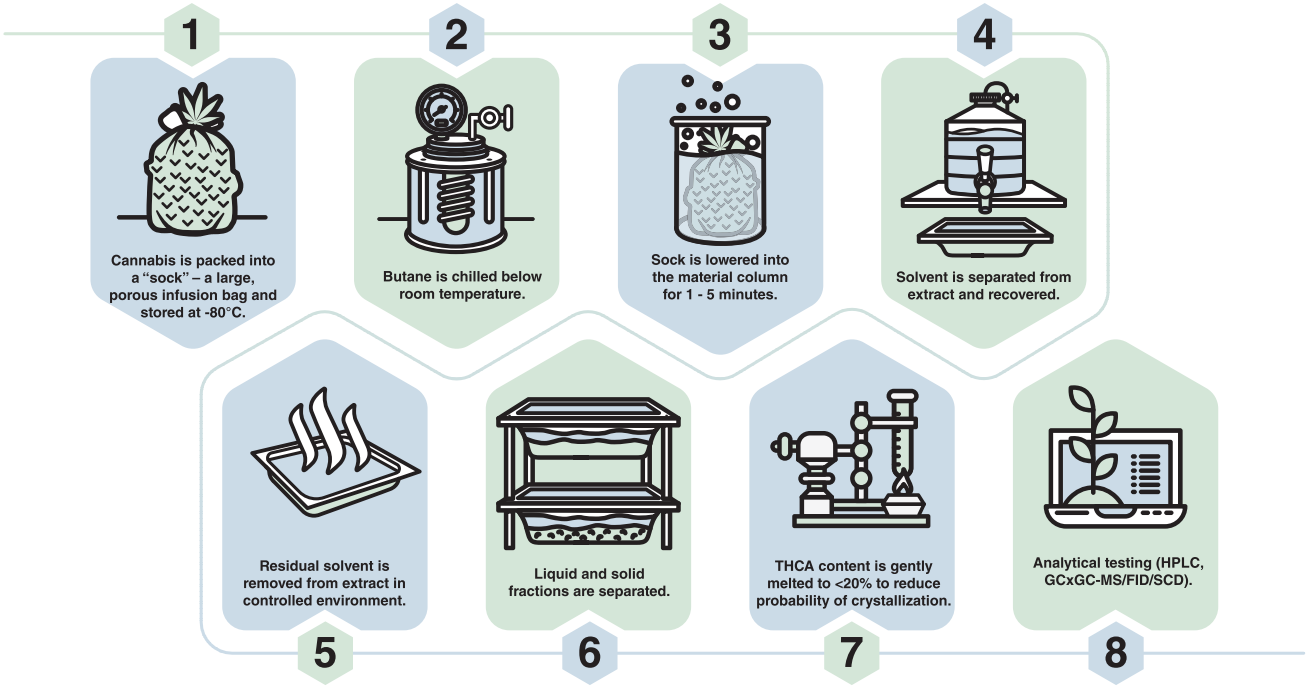

Figure 1. Workflow illustrating a general extraction process for creating cannabis extracts and further separating high terpene extracts (HTE). This method uses mild processing conditions to produce a concentrated extract, preserving a rich terpene profile and maintaining high cannabinoid and aroma concentrations. Key steps include subzero storage of biomass, low-temperature liquid butane extraction, solvent recovery, and analytical testing for quality control. The figure represents a generalized workflow rather than exact experimental parameters used in the study. Specific conditions employed in the experiments described here are detailed in Experimental section.

terpenes are routinely profiled for potency and aroma, the ancillary fraction remains poorly characterized despite its potential influence on chemical and physical properties and on the perceived quality of a given product.

The chemical diversity of nonpolar secondary metabolites produced by cannabis makes it well suited to extraction with organic solvents.[7] Industrial cannabis extraction has evolved over time, with ethanol among the earliest large-scale methods employed.[8] Ethanol provides broad solvation across both polar and nonpolar constituents (often marketed as Rick Simpson Oil, RSO) and is widely used in food-grade manufacturing. However, the coextraction of chlorophyll, polyphenols, waxes, and other polar compounds necessitates extensive downstream purification and imparts undesirable color and off-flavors, limiting its use for inhalable products.[7,9,10] Furthermore, ethanol's boiling point (78 °C) and high vapor pressure at moderate temperatures overlap with the volatility range of many cannabis aroma compounds, complicating solvent removal without significant loss or alteration of terpenes and other odor-active volatiles. For these reasons, ethanol extracts are now used primarily in oral or topical applications such as gummies and tinctures or in refined high-concentration cannabinoid products such as distillate.

Supercritical and later subcritical CO_2 subsequently emerged as a green, more advanced alternative, widely used in decaffeination, hop-oil recovery, and botanical essential-oil production owing to its tunable density, gas-like diffusivity, and minimal, nontoxic solvent residues.[11−14] Under typical pressures and temperatures, however, its low chemical selectivity results in coextraction of appreciable amounts of both polar and nonpolar species, including waxes, chlorophyll, pigments, and other lipophilic impurities, necessitating cosolvent modifiers and additional downstream refinement to achieve the purity required for vape applications.[8]

Over the past decade, hydrocarbon extraction, commonly referred to as Butane Hash Oil (BHO), using solvents such as *n*-butane, iso-butane, or propane, has become the dominant method for producing inhalable-grade non-distilled concentrates.[13] These nonpolar solvents selectively dissolve cannabinoids and aroma compounds while largely excluding chlorophyll and other more polar impurities, yielding high-purity oils with native-like sensory profiles. The high volatility of these hydrocarbons further enables solvent removal under mild conditions, minimizing loss of volatile compounds that contribute to aroma and flavor.

Nonetheless, hydrocarbon extracts, similar to those derived from CO_2 or ethanol, often contain a material referred to as "fats, lipids, and waxes" within the cannabis industry, manifesting as a solid or cloudy precipitate upon exposure to polar solvents (e.g., ethanol) during winterization and indicating the presence of highly nonpolar constituents. Despite its routine observation in commercial BHO production, the molecular identity of this wax fraction in hydrocarbon extracts remains poorly defined. Quantitative data linking extraction process variables, such as temperature, to final wax concentration are similarly underexplored. Equally unexamined is whether these nonvolatile constituents transfer into the aerosol phase during vaporization, where they could contribute to consumer inhalation exposure. Addressing these gaps is critical for optimizing hydrocarbon extraction conditions, ensuring product consistency, and evaluating the potential implications of wax-derived compounds for vape device performance and aerosol characteristics.

Shown in Figure 1 is a generalized industrial cannabis hydrocarbon extraction workflow. Frozen biomass is typically

https://doi.org/10.1021/acsomega.5c13451
ACS Omega XXXX, XXX, XXX−XXX

contacted with chilled liquid hydrocarbons such as *n*-butane to selectively dissolve cannabinoids and volatile aroma compounds. The resulting butane-rich solution is decanted and the solvent removed under mild conditions to yield a concentrated extract. Subsequent processing steps, including controlled heating and crystallization, are often used to separate THCA-rich fractions from the remaining liquid high terpene extract (HTE).

While long-chain *n*-alkanes have been previously identified as major constituents of cannabis wax byproducts generated during ethanol extraction and winterization, their temperature-dependent incorporation into bulk hydrocarbon extracts and subsequent transfer into mainstream Electronic Cannabinoid Delivery System (ECDS) aerosol have not been previously investigated.[15,16] To better understand the chemical makeup of HTE and the associated "fats and waxes" fraction, we performed a controlled evaluation of *n*-butane extraction across −46 to −9 °C using two chemotypically distinct cannabis cultivars.[17] For comparison, we also prepared an ethanol extract under typical production conditions. By using GC×GC−TOF−MS/FID, we identify long-chain *n*-alkanes (C_{22}−C_{31}; key examples summarized in Table 1) as major constituents of the ancillary wax fraction of hydrocarbon extracts whose abundance increases systematically with extraction temperature. In contrast, cannabinoid and aroma profiles remain largely constant over the same temperature range.[18,19]

Table 1. Key Long-Chain *n*-Alkanes and Select Properties Found in Hydrocarbon Extracts

Compound	Formula	MW (g/mol)	Melting Point (°C)
Pentacosane	$C_{25}H_{52}$	352	53−55
Hexacosane	$C_{26}H_{54}$	366	56−59
Heptacosane	$C_{27}H_{56}$	380	59−61
Octacosane	$C_{28}H_{58}$	394	61−64
Nonacosane	$C_{29}H_{60}$	408	63−66
Triacontane	$C_{30}H_{62}$	422	65−68
Hentriacontane	$C_{31}H_{64}$	436	68−70

Rheological analysis was then conducted to assess how these wax-derived alkanes influence viscosity, which governs flowability and strongly impacts vape device performance. Only small changes in apparent viscosity at 45 °C were observed, suggesting minimal influence of this chemical class on bulk rheology at the concentrations studied. Finally, we investigated the mass transfer of these compounds into mainstream Electronic Cannabinoid Delivery System (ECDS) or "vape" aerosols. Long-chain alkanes were efficiently transferred into the mainstream aerosol, and their concentrations mirrored the temperature-dependent trends observed in the raw extracts. Collectively, these findings implicate long-chain *n*-alkanes as an important but previously underappreciated chemical class in vape-ready extracts and establish hydrocarbon extraction temperature as a critical process parameter for minimizing wax coextraction while preserving cannabinoids and terpenes.

EXPERIMENTAL SECTION

Sample Procurement

Fresh-frozen cannabis inflorescence (40 lb each of the varieties GMO and Oreoz) was obtained from Pro Farms (License CDPH-10004721) and stored at −50 °C to minimize degradation of volatile and nonvolatile constituents. Extractions were performed in 2023 at Abstrax Laboratories, a Type 7 licensed cannabis facility in California.

Cannabis Hydrocarbon Extraction

Extractions were performed using an ExtractionTek stainless-steel hydrocarbon system with liquid *n*-butane as the solvent. Prior to use, the system was flushed with solvent to remove residual contaminants. Approximately 10 lb (≈4.54 kg) of fresh-frozen cannabis of a given variety were packed into 100 μm mesh extraction socks and stored at −50 °C. The extraction column and *n*-butane solvent tank were chilled to the target experimental temperature (−9, −32, or −46 °C), corresponding to approximately 15, −25, and −50 °F, which reflect common industrial operating set points. The porous mesh sock, maintained at −50 °C, was loaded into the extraction column, and a system-wide vacuum was applied.

Extraction was performed in two passes: a primary pass using approximately 20 lb (≈9.1 kg) of liquid *n*-butane, followed by a secondary pass using approximately 5 lb (≈2.3 kg), yielding a total solvent volume of approximately 25 lb (≈11.4 kg) per 10 lb biomass run, corresponding to a solvent-to-biomass ratio of approximately 2.5:1 (w/w).

Cooled *n*-butane was then injected into the extraction column using nitrogen pressure (≈15−45 psi) and allowed to soak the biomass for 3 min per pass. Nitrogen (≈40−100 psi) was subsequently used to drain the column and facilitate solvent transfer through an inline stainless-steel particulate filter (0.5 μm nominal pore size) prior to solvent recovery. This filtration step serves only to remove suspended plant particulates from the solvent stream. No adsorbent filtration media (e.g., clays, silica, or other chromatographic materials) were used, and the filter was not intended to selectively remove dissolved chemical constituents. Solvent recovery of *n*-butane was then performed, and the crude extract was collected.

The extract was placed in an oven at 30 °C to remove residual *n*-butane to initiate crystal nucleation of the THCA fraction, with the material stirred every 8 h for 48 h to promote crystal growth. The liquid HTE fraction was separated and heated at 60 °C for 4 h to partially decarboxylate residual THCA. Cannabinoid composition, including THCA and Δ^9-THC, was quantified by HPLC-DAD using external calibration standards as described below. Samples were placed in glass jars that were loosely capped to minimize contamination while allowing limited venting during heating. Under these conditions, THCA content was reduced to <20% of the total cannabinoid fraction (Table S5). Terpene concentrations were not specifically monitored during this heating step as part of the present experiment; however, the relatively mild temperature and short heating duration are consistent with conditions commonly used in industry to induce partial decarboxylation while limiting volatilization losses.

To minimize the possibility of cross-contamination between samples, two independent extraction columns were used, with each cultivar processed on a dedicated system. Between extraction runs, the hydrocarbon extraction system was flushed with fresh solvent as part of the standard operating procedure prior to initiating the next extraction. Additionally, the butane solvent used for extraction was independently analyzed to confirm purity and absence of detectable contaminants prior to use. These measures reduce the likelihood that residual material from prior runs could influence extract composition.

Winterization of HTE

Winterization of HTE samples was performed by dissolving crude extracts in methanol (20 mL per gram of HTE) and cooling to −50 °C. The resulting precipitate was collected by vacuum filtration and washed with cold methanol (−50 °C) to yield an off-white, powdery solid, hereafter referred to as the crude wax fraction. The crude wax fraction was analyzed by direct liquid injection using GC×GC−TOF−MS/FID.

Ethanol Extraction

Five pounds (≈2.3 kg) of fresh-frozen cannabis (GMO or Oreoz) were submerged in 200-proof ethanol (2 L) and stored at −50 °C for 1 h. The mixture was then filtered to remove solid plant material, and

https://doi.org/10.1021/acsomega.5c13451
ACS Omega XXXX, XXX, XXX−XXX

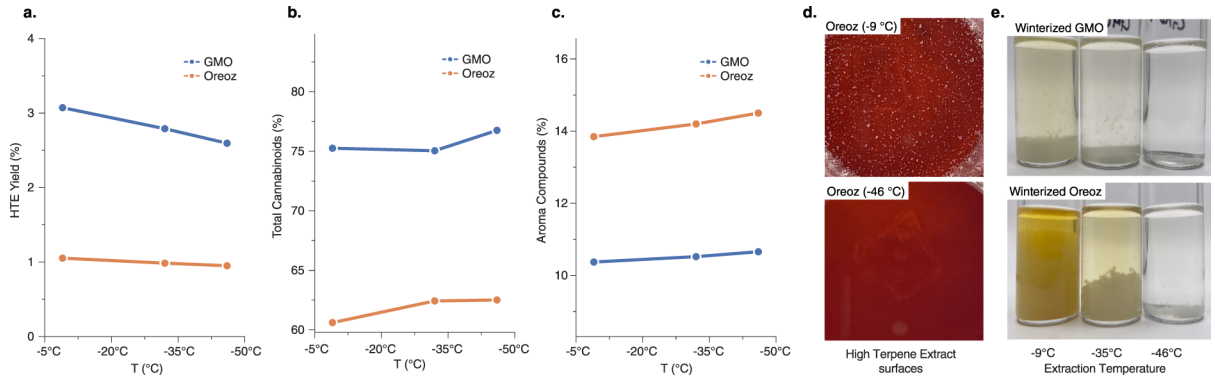

Figure 2. Impact of extraction temperature on HTE yield, composition, and visible wax precipitation. **a.** High terpene extract (HTE) yield (wt %) for GMO and Oreoz as a function of *n*-butane extraction temperature (−9, −32, −46 °C). **b.** Total cannabinoids (HPLC-DAD) expressed as wt % of the HTE. **c.** Total quantified aroma compounds (GC×GC−TOF−MS/FID) expressed as wt % of the HTE. **d.** Photographs of Oreoz HTE produced at −9 °C (top) and −46 °C (bottom), showing visible white speckling at the warmer extraction condition consistent with coextracted waxes. **e.** Winterized GMO (top row) and Oreoz (bottom row) HTE after methanol winterization at −50 °C (20 mL methanol to 1 g HTE), illustrating the progressive decrease in off-white wax precipitate from −9 to −46 °C.

the ethanol was evaporated under vacuum using a rotary evaporator to obtain a concentrated crude extract.

High-Performance Liquid Chromatography with Diode Array Detector (HPLC-DAD)

Cannabinoid quantification was performed using an Agilent 1200 high-performance liquid chromatograph (HPLC) equipped with a diode array detector (DAD) set to 228 nm. A mixed cannabinoid standard (500 ppm, Cerilliant) was purchased from Sigma-Aldrich and diluted in methanol to generate external calibration curves (Table S4).

For sample preparation, HTE (0.200 ± 0.050 g) was dissolved in 50 mL of methanol and sonicated to ensure complete dissolution. After cooling to room temperature, a secondary dilution was prepared by diluting 100 μL of the primary solution to 1.00 mL with methanol.

Separation was achieved on a Restek Raptor ARC-18 column (3.0 × 100 mm, 1.8 μm) using a mobile phase of solvent A (water +5 mM ammonium formate +0.1% formic acid) and solvent B (acetonitrile +0.1% formic acid). The method was isocratic at 28% A and 72% B, with a flow rate of 0.8 mL/min at 30 °C. Cannabinoid concentrations were determined by external calibration, and data were processed using Agilent ChemStation CDS software. Instrument parameters are found in Table S3.

Comprehensive Two-Dimensional Gas Chromatography

GC×GC analyses were performed using an Agilent 7890B gas chromatograph equipped with an INSIGHT reverse fill−flush flow modulator (SepSolve Analytical). The primary separation used a BPX5 column (20 m × 0.18 mm ID × 0.18 μm), and the secondary separation used a Mega Wax HT column (4.8 m × 0.32 mm ID × 0.25 μm). Detection was achieved with a BenchTOF2 time-of-flight mass spectrometer (TOF-MS) and a flame ionization detector (FID) operated in parallel. Samples were introduced using liquid injection with an Agilent 7693 autosampler (G4513A) with a 3 μL injection volume. The inlet temperature was maintained at 280 °C with a 20:1 split ratio for all analyses. TOF-MS was used for compound identification, while quantitation was based exclusively on FID response, with conditions summarized in Table S1.

All samples were prepared by dissolving material in 4.0 mL of hexanes, followed by filtration through a Linktor 25 mm, 0.22 μm PTFE syringe filter and transfer into 2 mL autosampler vials. Sample masses were 0.120 ± 0.025 g for hydrocarbon-extracted (HTE) samples, 0.30 ± 0.02 g for fresh frozen inflorescence, and 0.120 ± 0.025 g for ethanol-extracted samples. All HTE samples were analyzed in analytical triplicate (n = 3 independent GC×GC injections) to assess analytical reproducibility; reported concentrations are expressed as mean ± SD.

The oven temperature program was: 45 °C (3 min), ramp 3 °C/min to 98 °C, 5 °C/min to 140 °C, 3 °C/min to 175 °C, 2 °C/min to 200 °C, then 15 °C/min to 270 °C (28 min hold). The modulation period was 6.0 s.

Data was acquired, integrated, and processed using ChromSpace software (SepSolve Analytical). Statistical analyses, including principal component analysis (PCA) and correlation analysis, were performed in Python 3 (NumPy, pandas, SciPy). GC×GC chromatograms were aligned to correct for a 2.5 s void time in the second dimension. Representative chromatograms of HTE samples are shown in Figures S3 and S4.

Quantitative analysis was performed using external calibration with flame ionization detector (FID) response. Authentic terpene standards and a custom flavorant standard mixture were obtained from LGC Standards (Manchester, NH, USA). Linear retention index (LRI) calibration was performed using an *n*-alkane standard mixture (C_7−C_{40}; Sigma-Aldrich, St. Louis, MO, USA). In addition, an in-house custom standard mixture was prepared to extend calibration coverage for select analytes not available commercially (Table S2).

Calibration solutions were prepared in hexanes at multiple concentration levels spanning the expected analyte ranges in the samples. Calibration curves were generated by plotting FID response versus concentration, and linear regression was used to determine response factors. Calibration statistics, including coefficients of determination (R^2), are summarized in Table S2.

Viscosity Analysis

Dynamic viscosity was measured using a microfluidic capillary viscometer (microVISC, RheoSense Inc.) equipped with a VROC measurement cell. Samples (≈100 μL per run) were loaded into disposable syringes and equilibrated at 45 °C using the instrument's integrated temperature control (±0.1 °C) for 5 min prior to measurement. The viscometer was verified with viscosity standards spanning the expected sample range. For each sample, three independent measurements were collected at stepped flow rates to confirm behavior (flow-rate invariance within ±3%), with conditions shown in Table S6. Between samples, the flow path was flushed with isopropanol and inspected for absence of air bubbles; at the end of each session, the system was cleaned per the manufacturer's protocol.

Aerosol Mass Transfer Analysis

Aerosol capture experiments were conducted to determine whether the identified long-chain *n*-alkanes transfer into the mainstream aerosol generated during vaping. We selected industry-standard, all-ceramic 510 cartridges coupled to a puff machine. Vape cartridges (0.5 g fill) were filled with HTE oils and attached to a multichannel CH Tech puffing system calibrated to emulate human inhalation topography. Each cartridge was subjected to a standardized 60-puff

https://doi.org/10.1021/acsomega.5c13451
ACS Omega XXXX, XXX, XXX−XXX

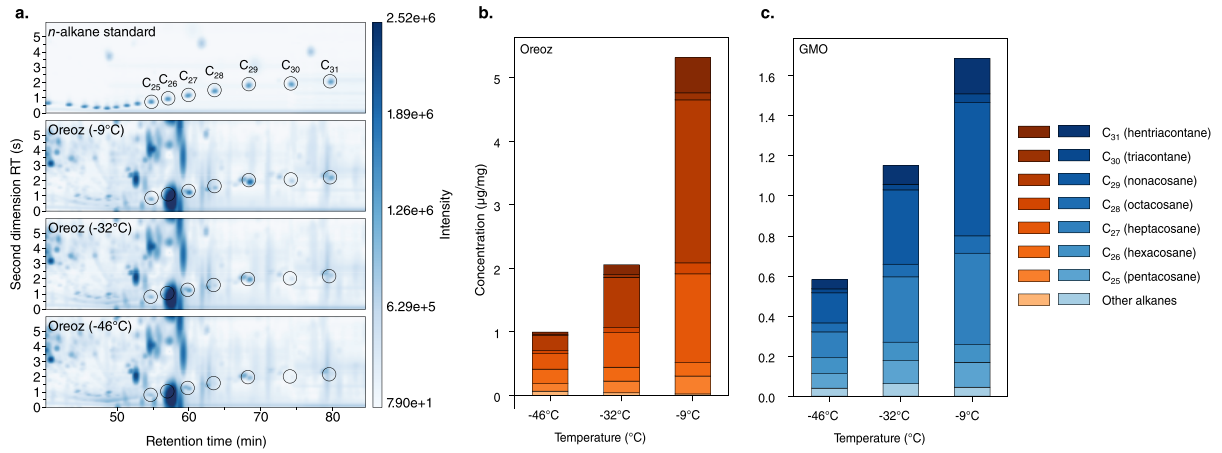

Figure 3. a. GC×GC−FID chromatograms of an *n*-alkane standard and the representative Oreoz samples extracted at different temperatures. The chromatographic region shown is focused on the late eluting wax region, with the major alkanes annotated. **b.** Average alkane concentrations for Oreoz at each extraction temperature. **c.** Average alkane concentrations for GMO at each extraction temperature.

regimen, representing the cumulative aerosol output over a typical 0.5 g cartridge lifetime.

Aerosol sampling was conducted in quadruplicate (n = 4 independent cartridges) for each variety−temperature condition. Each channel was calibrated every 20 puffs to a flow rate of 3 standard liters per minute (SLPM) using an Alicat Whisper mass flow meter. The electronic cannabis delivery system (ECDS) consisted of Active Alpha 510 batteries (configured for straight-voltage nonmodulated output) powering Active 0.5 mL Easy Click Ceramic Pro 510 cartridges. Batteries were fully charged and replaced as needed to maintain a constant 3.5 V output.

The mass of each filled ECDS was recorded before and after each 20-puff block. Aerosol was collected on 47 mm Cambridge glass fiber filter pads (CFPs) placed inline 5 in. downstream of the ECDS mainstream emissions point. Three CFPs per cartridge, each collecting 20 puffs, were weighed individually and then combined for extraction. Prior to testing, new tubing was installed in the aerosol path and existing tubing was inspected to ensure minimal flow impedance. Average aerosol capture efficiency across all conditions was ≈84% (Table S10).

The captured aerosol on combined filter pads was prepared for liquid-injection GC×GC-TOF-MS/FID analysis by extracting the retained oil with 6 mL of hexanes with vigorous agitation for 5 min followed by filtration. Wax concentrations were expressed as μg wax per mg aerosol, normalized to total cart-depleted mass (the mass lost from the cartridge over 60 puffs) rather than pad-collected mass, to provide a denominator independent of capture efficiency. Representative GMO and Oreoz aerosol chromatograms are shown in Figures S6 and S7.

RESULTS

Impact of Extraction Temperature on Wax Composition

Hydrocarbon extraction with *n*-butane was performed on two cannabis cultivars, GMO and Oreoz, at −9, −32, and −46 °C. After separation of crystalline THCA, the remaining liquid fraction, referred to as the high terpene extract (HTE), decreased in yield with decreasing extraction temperature (Figure 2a). At −9 °C, GMO produced ≈3 wt % HTE compared to ≈1.1 wt % for Oreoz, and the −46 °C condition yielded the lowest HTE mass for both cultivars, consistent with reduced solubility at colder temperatures.

Winterization of the HTE samples produced an off-white precipitate (Figure 2e), with larger quantities observed in extracts produced at higher temperatures, indicating that increased coextraction of this wax fraction likely contributes to the moderate increase in yield under warmer conditions. GC×GC−TOF−MS/FID analysis of the crude wax fraction revealed that the monoterpene and sesquiterpene regions of the chromatogram were essentially free of peaks. Instead, a series of periodically spaced, late-eluting peaks extending from the cannabinoid region to longer first-dimension retention times and low second-dimension retention times was observed, consistent with very nonpolar species.[16]

HPLC-DAD was then used to characterize cannabinoids in the crude wax fraction. THCA was present at the highest concentrations (∼17%), indicating that THCA has limited solubility in methanol at −50 °C and can coprecipitate with the wax fraction. This behavior should be considered when applying winterization in industrial settings to minimize cannabinoid loss.

To obtain a refined wax fraction, the crude wax fraction was subjected to column chromatography on silica 60 using hexane:ethyl acetate (80:20) as the eluent that provided an R_F of 0.5 (Figure S1). The resulting purified wax fraction was a white, flaky solid whose GC×GC−TOF−MS chromatogram was dominated by the late-eluting nonpolar series. Time-of-flight mass spectra of these peaks identified them as *n*-alkanes with molecular masses ≥ 310 Da corresponding to C_{22}−C_{31} homologues. Additional low-intensity peaks coeluting in the same second-dimension region suggested the presence of branched aliphatic hydrocarbons (e.g., iso-alkanes), although their identities remain tentative in the absence of standards. The major *n*-alkane peaks were confirmed by comparison with an *n*-alkane reference mixture, with heptacosane ($C_{27}H_{56}$) and nonacosane ($C_{29}H_{60}$) detected at the highest concentrations, with additional contributions from pentacosane, triacontane, and hentriacontane.

These *n*-alkanes are well-documented constituents of plant epicuticular waxes, where they form a hydrophobic protective layer on leaves, stems, and inflorescences.[20,21] In all HTE samples, heptacosane and nonacosane were the most abundant homologues, consistent with prior reports of long-chain *n*-alkanes in plant cuticular waxes, including CBD-rich hemp.[21,22]

After assigning the composition of the purified wax fraction, we quantified these *n*-alkanes in the original HTE samples. Figure 3a compares the GC×GC−TOF−MS chromatograms of an *n*-alkane standard (C_7−C_{40}) and the wax/cannabinoid region (40−80 min) for the Oreoz extracts. The absence of *n*-

https://doi.org/10.1021/acsomega.5c13451
ACS Omega XXXX, XXX, XXX−XXX

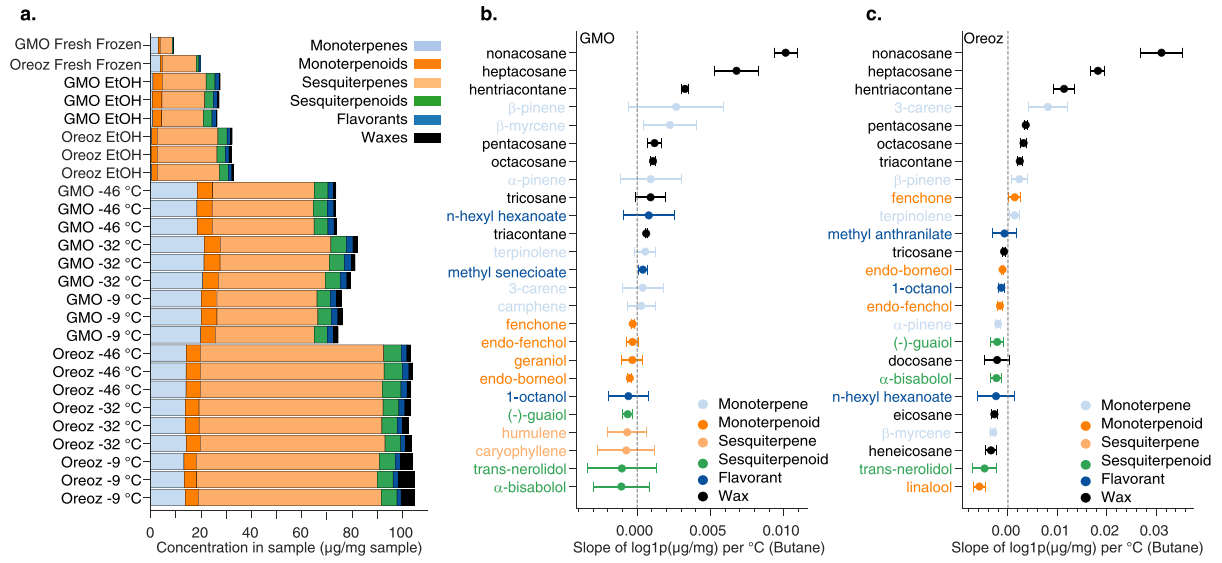

Figure 4. Temperature dependence of volatile classes and individual analytes in extracts. **a.** Stacked horizontal bar plots showing the concentration contributed by each chemical class (monoterpenes, monoterpenoids, sesquiterpenes, sesquiterpenoids, other flavorants, and waxes) for fresh-frozen inflorescence, ethanol extracts, and butane extracts (HTE) from GMO and Oreoz. Replicates are shown for each condition. Across butane HTEs (−46, −32, −9 °C), class distributions are dominated by terpene/terpenoid classes and remain broadly consistent with extraction temperature, while wax abundance increases at warmer conditions. (**b, c**) Temperature sensitivity expressed as the slope of $\log_{10}$ (µg/mg) versus extraction temperature for representative compounds, estimated from butane HTE data for **b.** GMO and **c.** Oreoz. Points denote fitted slopes with 95% confidence intervals; colors indicate compound class. Most monoterpenes, terpenoids, and flavorants exhibit slopes near zero (minimal temperature dependence), whereas long-chain *n*-alkanes show consistently positive slopes, indicating increased wax co-extraction at higher temperatures.

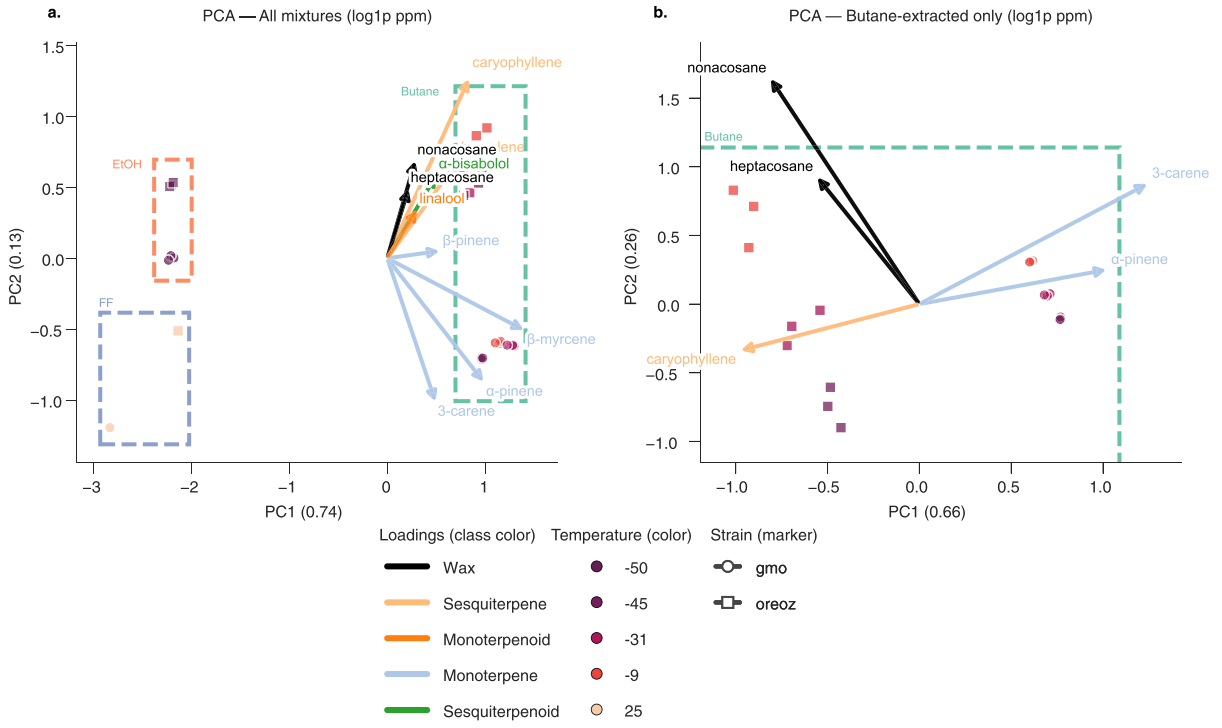

Figure 5. a. Principal component analysis (PCA) of volatile and wax composition in cannabis extracts (ethanol and butane derived) and fresh frozen flower (FF). Scores and loadings plots based on ln(1+ppm) concentrations of quantified analytes, colored by chemical class (waxes, monoterpenes, sesquiterpenes, monoterpenoids, sesquiterpenoids). **b.** In the HTE-only PCA, variation with extraction temperature is driven primarily along a wax-associated dimension (PC2), while terpenes differentiate the two varieties primarily along the first principal component.

alkane peaks in the procedural blank confirmed that the observed alkane signals were intrinsic to the samples rather than analytical background or contamination (Figure S2).

A systematic decrease in *n*-alkane peak intensity with decreasing extraction temperature paralleled the reduced mass of winterized precipitate, reinforcing the link between extraction conditions and coextraction of epicuticular waxes. Quantitation using external *n*-alkane standards confirmed these trends in both cultivars (Figure 3b and c).

https://doi.org/10.1021/acsomega.5c13451
ACS Omega XXXX, XXX, XXX−XXX

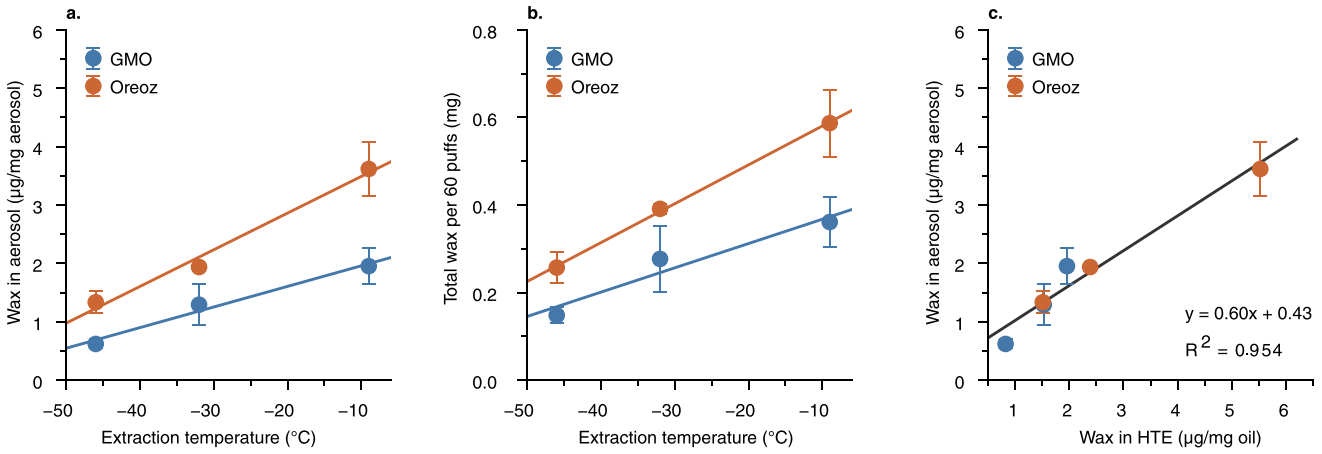

Figure 6. Aerosolized epicuticular wax *n*-alkanes as a function of extraction temperature and HTE composition. **a.** Wax concentration in mainstream aerosol (μg/mg aerosol) for GMO and Oreoz HTE vapes produced at −46, −32, and −9 °C. **b.** Total wax mass delivered over a standardized 60-puff protocol for the same cartridges, with four replicates per HTE. **c.** Relationship between wax content in the starting HTE (μg/mg oil) and wax in the aerosol (μg/mg aerosol), showing an approximately linear correlation (R^2 = 0.954) across both varieties.

Impact of Extraction Temperature on Cannabinoid and VOC Composition

Targeted GC×GC-TOF-MS/FID analysis was then performed to quantify the volatile aroma fraction. The method employed multiple external calibration analyte sets including common terpenes, nonterpenoid flavorants, and *n*-alkanes (analytes shown in Table S2). Total quantified volatiles showed only small temperature-dependent changes (Figure 2b). For GMO, volatiles increased from ≈10 to ≈11 wt % between −9 and −46 °C, whereas Oreoz increased from ≈13.9 to ≈14.5 wt %. Thus, lowering extraction temperature slightly enriches the volatile fraction, but these changes are on the order of a few percent of the total extract mass.

To examine whether lower temperatures selectively enrich particular volatile classes, we grouped analytes into monoterpenes, monoterpenoids, sesquiterpenes, sesquiterpenoids, and other flavorants (i.e., nonterpene volatiles). Stacked horizontal bar charts (Figure 4a) show that sesquiterpenes and sesquiterpenoids dominate the quantified volatile profile for both varieties at all temperatures, with monoterpenes and monoterpenoids comprising a smaller but consistent fraction. The relative contribution of each class is fairly stable across −46 to −9 °C, with no systematic shift from monoterpenes toward higher-boiling sesquiterpenes at warmer conditions.

We next quantified temperature sensitivity at the level of individual analytes by fitting a simple linear model to each compound across the three butane extraction temperatures for a given variety. For each analyte we regressed $\log_{10}[1+C]$ (μg analyte per mg HTE) against extraction temperature (°C) and extracted the slope (β_1) and its 95% confidence interval. Figure 4b and c plot these slopes for GMO and Oreoz, respectively, where positive values indicate increasing abundance with higher extraction temperature and the vertical dashed line denotes zero effect.

In both cultivars, the long-chain *n*-alkanes, especially nonacosane, heptacosane, and hentriacontane, show the largest positive slopes, with narrow confidence intervals that do not overlap zero. This confirms that these high-MW wax constituents are enriched as extraction temperature increases, consistent with their limited solubility at low temperatures and the greater ability of warmer, less viscous *n*-butane to dissolve epicuticular wax domains.

By contrast, most monoterpenes, sesquiterpenes, and flavorants cluster close to the zero-slope line, with confidence intervals that span zero or only modestly deviate from it. A few individual terpenoids and esters exhibit small positive slopes, but their temperature dependence is weak compared to that of the *n*-alkanes. Together with the class-level data in Figure 4a, these slope plots show that within the tested window, extraction temperature has a disproportionately strong effect on the large *n*-alkane waxes, while leaving the concentrations of most aroma-active VOCs comparatively insensitive.

Finally, principal component analysis (PCA) of log-transformed volatile concentrations was used to compare chemical fidelity across extraction methods (Figure 5a). When all sample types were included (HTE, ethanol extracts, and fresh frozen inflorescence), loadings indicated that monoterpenes and monoterpenoids (e.g., α-pinene, β-myrcene, linalool, caryophyllene) drive the separation between inflorescence-like samples and ethanol extracts, while long-chain alkanes and higher-boiling constituents contribute along an orthogonal direction. When the PCA was restricted to HTE samples only (Figure 5b), extracts clustered by variety with shifts along PC1 and PC2 as a function of temperature, reinforcing that the overall volatile composition of HTE is largely conserved across the −46 to −9 °C range.[23]

Collectively, these results show that *n*-butane extraction across typical subzero process temperatures yields HTE with nearly invariant cannabinoid and volatile profiles, while wax content is strongly temperature-dependent. Lowering the extraction temperature therefore offers a pragmatic route to reduce coextracted waxes without materially distorting the aroma fingerprint relative to the starting inflorescence.

Viscosity Analysis

Viscosity is a critical parameter for vape performance because it governs how reliably oil wicks into the cartridge, how efficiently it aerosolizes, and whether devices flood or run dry under typical use. We therefore measured the viscosity at 45 °C of the butane-extracted HTE samples and found that Oreoz consistently exhibited lower viscosity than GMO, with average values of 870−970 mPa·s vs 2,160−2,490 mPa·s, respectively (Table S7). Despite the pronounced temperature dependence of wax concentration in the extracts, only modest changes in viscosity were observed across the extraction series

https://doi.org/10.1021/acsomega.5c13451
ACS Omega XXXX, XXX, XXX−XXX

for each variety (~10% for Oreoz, ~13% for GMO across the full −9 to −46 °C extraction range), and no strong monotonic trend with extraction temperature emerged. This suggests that bulk rheology is dominated by the cannabinoid/terpene matrix rather than the relatively small epicuticular wax fraction, and the lower viscosity of Oreoz is consistent with its higher volatile fraction and lower total cannabinoid content.

Aerosolization of Epicuticular Wax *n*-Alkanes During Vaping

Aerosol capture experiments were conducted to determine whether the long-chain *n*-alkanes identified in the wax fraction are transferred into the mainstream aerosol during vaping. High terpene extracts produced at each extraction temperature were filled into 0.5 g cartridges and connected to a puffing machine calibrated to emulate human inhalation patterns. Cartridges were vaped under a standardized 60-puff protocol (n = 4 independent cartridges per condition), with aerosol from three consecutive 20-puff blocks collected on separate Cambridge filter pads and subsequently combined per cartridge for quantitation (Figure S5).

GC×GC-TOF-MS/FID analysis of the pad extracts revealed the same series of long-chain *n*-alkanes previously identified in the purified wax fraction, confirming that these epicuticular wax constituents are entrained into the aerosol despite their high molecular weights and low vapor pressures.[24] For each cartridge, total wax collected on all pads was summed and normalized to the total cart-depleted mass to obtain a wax concentration (μg wax per mg cart-depleted aerosol), and was also expressed as total wax mass delivered per 60-puff run (Figure 6a,b).

For Oreoz, aerosol wax concentrations increased systematically with extraction temperature, from 1.33 ± 0.19 μg/mg at −46 °C to 1.94 ± 0.05 μg/mg at −32 °C and 3.62 ± 0.47 μg/mg at −9 °C, corresponding to a 2.7-fold increase between the coldest and warmest conditions (Figure 6a). GMO displayed the same qualitative trend at lower absolute levels, with aerosol wax concentrations of 0.62 ± 0.08 μg/mg at −46 °C, 1.29 ± 0.35 μg/mg at −32 °C, and 1.95 ± 0.31 μg/mg at −9 °C—a 3.2-fold increase across the tested temperature range. On a dose-normalized basis, this corresponds to wax exposure increasing from ≈0.13 to ≈0.36 mg wax per 100 mg aerosol for Oreoz and from ≈0.06 to ≈0.20 mg per 100 mg aerosol for GMO when comparing −46 and −9 °C.

Total wax mass delivered over the 60-puff protocol also depended strongly on extraction temperature (Figure 6b). For Oreoz, the combined pads contained ≈0.27 mg wax at −46 °C and ≈0.59 mg at −9 °C (≈2.2-fold increase), whereas GMO increased from ≈0.15 mg at −46 °C to ≈0.38 mg at −9 °C (≈2.5-fold increase). Across both varieties and all temperatures, Oreoz consistently delivered 1.5−2.2× more wax per mg aerosol than GMO, a difference attributable primarily to nonacosane (C_{29}) content in the Oreoz HTE (59.3 ± 14.0 ppm at −9 °C vs 19.9 ± 6.2 ppm for GMO).

Across all variety−temperature combinations, aerosol wax concentrations closely tracked the wax content of the starting HTE on a mass basis, with an approximately linear relationship between wax in the oil (μg/mg HTE) and wax in the aerosol (μg/mg aerosol; R^2 = 0.954; Figure 6c). The regression slope of 0.60 indicates that approximately 60% of HTE wax content is recoverable in the aerosol under these conditions, with the nonzero intercept (0.43 μg/mg) reflecting a residual baseline wax transfer that persists even in lower-wax extracts. These results demonstrate that long-chain *n*-alkanes present in cannabis extracts are readily carried into the mainstream aerosol during vaping, and that lowering the extraction temperature can markedly reduce wax levels in both the bulk HTE and the resulting aerosol.

DISCUSSION

This study demonstrates that extraction temperature exerts a strong influence on the extent to which epicuticular waxes are coextracted alongside desired phytochemicals during butane extraction of cannabis concentrates. As shown in Figure 2, lowering the extraction temperature modestly reduces HTE yield but has only minor effects on total cannabinoids and total quantified aroma compounds, which remain within a relatively narrow range across −46 to −9 °C for both cultivars. This likely explains why extraction temperature has historically received less scrutiny with respect to potency and aroma, despite its pronounced impact on wax content.

In contrast, the long-chain alkanes assigned as epicuticular wax constituents show a clear, temperature-dependent enrichment, as highlighted in the slope analysis shown in Figure 4b and c. GC×GC-TOF-MS/FID analysis of the winterized fractions and quantitation of individual *n*-alkane homologues reveal that C_{22}−C_{31} alkanes increase systematically with extraction temperature in both varieties, with heptacosane and nonacosane dominating the series. While prior work has characterized *n*-alkanes in isolated wax byproducts from ethanol extraction,[15,16] the present study is the first to quantify their temperature-dependent coextraction into bulk hydrocarbon HTE and to demonstrate their transfer into mainstream aerosol. These hydrocarbons, which naturally coat the surface of cannabis inflorescences, are more readily solubilized under warmer extraction conditions, likely due to reduced solvent viscosity, increased diffusivity, and enhanced disruption of the cuticular layer.[22,25] This provides a mechanistic basis for the long-standing empirical practice of using subzero hydrocarbon extraction and clarifies that temperature primarily modulates coextraction of epicuticular waxes rather than the desired cannabinoids or terpenes.

Despite the clear differences in wax loading, the impact on bulk rheology at 45 °C was modest (Table S7). In the high terpene extracts studied here, cannabinoids and terpenes dominate the mass balance, so changes of a few milligrams of wax per 0.5 g cartridge lead only to incremental changes in apparent viscosity. From a processing standpoint, this suggests that texture or flow alone may not be a sensitive indicator of wax contamination in HTE formulations.

The aerosol experiments, however, show that relatively small changes in wax content can translate into measurable differences in aerosolized wax dose. As summarized in Figure 6a, aerosol wax concentrations (μg/mg aerosol) increase with extraction temperature in parallel with wax levels in the starting HTE, and Figure 6b illustrates the associated changes in total wax mass delivered over a standardized 60-puff run. Oreoz exhibits roughly a ≈2.7-fold reduction in aerosolized wax when moving from −9 to −46 °C, while GMO shows a ≈3.2-fold reduction over the same temperature range. The approximately linear relationship between wax in the oil and wax in the aerosol (R^2 = 0.954; Figure 6c) indicates that vaping carries these *n*-alkanes forward into the mainstream aerosol in approximate proportion to their initial abundance.

The toxicological implications of inhaling plant-derived long-chain *n*-alkanes remain poorly defined, particularly under

https://doi.org/10.1021/acsomega.5c13451
ACS Omega XXXX, XXX, XXX−XXX

chronic, low-level exposure scenarios typical of frequent vaping.[26] Future studies combining controlled aerosol generation and in vitro or in vivo exposure models will be important to more fully assess any safety concerns.

The volatile aroma data further highlights the selectivity of low-temperature *n*-butane extraction. Class-level analyses (Figure 4a) show that monoterpenes, sesquiterpenes, and other flavorants are only modestly affected by extraction temperature, with shifts that are much less pronounced than those observed for the wax fraction. Multivariate analysis by PCA (Figure 5a) reinforces this picture: Within the HTE sample clusters (Figure 5b), the samples partition by their extraction temperature, which is primarily due to heptacosane and nonacosane contributing to the PC2 direction. Together, these results indicate that low-temperature butane extraction preserves native-like aroma profiles while allowing substantial reductions in coextracted wax.

We last note that these wax-associated *n*-alkanes may be present in other extract form factors beyond hydrocarbon-derived extracts, including solventless rosin and high-THC refined products such as distillate or fully decarboxylated "liquid diamonds" (melted THCA). Because these materials can undergo markedly different thermal treatments and purification steps (e.g., short-path or wiped-film distillation, winterization, filtration), the resulting *n*-alkane levels are not obvious *a priori*. Future studies quantifying long-chain *n*-alkanes across common concentrate categories would help establish typical concentration ranges and identify which processing methodologies most effectively reduce them.[27]

CONCLUSIONS

We performed a series of temperature-dependent *n*-butane extractions of cannabis inflorescence to elucidate the composition and behavior of the "fats and waxes" fraction in high terpene extracts. Long-chain *n*-alkanes derived from the plant epicuticular wax layer were identified as the dominant wax constituents and were strongly dependent on extraction temperature, with the coldest condition yielding up to an approximately 3-fold reduction in alkane content relative to the warmest. In contrast, cannabinoids, volatile aroma compounds, and bulk viscosity showed only modest changes across the same temperature range, indicating that low-temperature butane extraction largely preserves the desired phytochemical and rheological properties of the oils. Aerosol capture experiments demonstrated that these *n*-alkanes are efficiently transferred into the mainstream aerosol during vaping, indicating that they should be considered in future inhalation toxicology evaluations. Taken together, our results establish extraction temperature as a powerful and practical process parameter for minimizing epicuticular wax coextraction, and the resulting aerosol wax dose, while maintaining cannabinoid and volatile profiles that remain closely aligned with the source cannabis material.

ASSOCIATED CONTENT

Supporting Information

The Supporting Information is available free of charge at https://pubs.acs.org/doi/10.1021/acsomega.5c13451.

HPLC-DAD calibration curve table; GC×GC-TOF-MS calibration curve table; GC×GC-TOF-MS chromatograms; aerosol experimental setup pictures (PDF)

AUTHOR INFORMATION

Corresponding Author

Iain W. H. Oswald − *Department of Research and Development, Abstrax Tech, Tustin, California 92780, United States;* orcid.org/0000-0002-5466-0405; Email: iain.oswald@abstraxtech.com

Authors

Manuel E. Sosa − *Department of Research and Development, Abstrax Tech, Tustin, California 92780, United States*

Twinkle R. Paryani − *Department of Research and Development, Abstrax Tech, Tustin, California 92780, United States*

Randy J. Reed − *Active, Seattle, Washington 98121, United States*

Alex W. Siegel − *Better Flange SPD, San Diego, California 92126, United States*

Qianxiang Ai − *Department of Research and Development, Abstrax Tech, Tustin, California 92780, United States*

Eugene Lee − *Department of Research and Development, Abstrax Tech, Tustin, California 92780, United States*

Daniel L. Radford − *Department of Research and Development, Abstrax Tech, Tustin, California 92780, United States*

Thomas J. Martin − *Department of Research and Development, Abstrax Tech, Tustin, California 92780, United States*

Kevin A. Koby − *Department of Research and Development, Abstrax Tech, Tustin, California 92780, United States*

Complete contact information is available at: https://pubs.acs.org/10.1021/acsomega.5c13451

Author Contributions

M.E.S. conceived and conducted the study, performed GC×GC experiments, and wrote the manuscript. T.R.P. assisted with GC×GC data collection. R.J.R. performed aerosol sampling. A.W.S. and K.A.K. provided extraction guidance and contributed to data interpretation. Q.A. performed data analysis. E.L. carried out extractions. D.L.R. acquired HPLC-DAD data. T.J.M. and I.W.H.O. oversaw and managed the project. All authors edited the manuscript and approved the final version.

Funding

This work was supported by Abstrax Tech, Inc., which funded the research and publication costs.

Notes

The authors declare the following competing financial interest(s): M.E.S., T.R.P, Q.A., E.L., D.L.R., T.J.M., K.A.K., and I.W.H.O. are employees of Abstrax Tech. R.J.R. is an employee of Active. A.W.S. is an employee of Better Flange SPD. The authors declare no other competing financial interest.

ACKNOWLEDGMENTS

The authors thank C. Rall and A. Real for their extraction expertise and M. V. Sosa for support and encouragement.

REFERENCES

(1) Potter, G. R.; Barratt, M. J.; Malm, A.; Bouchard, M.; Blok, T.; Christensen, A.-S.; Decorte, T.; Frank, V. A.; Hakkarainen, P.; Klein, A., et al. Global Patterns of Domestic Cannabis Cultivation: Sample

Characteristics and Patterns of Growing across Eleven Countries. In *Friendly Business: International Views on Social Supply, Self-Supply and Small-Scale Drug Dealing*; Werse, B.; Bernard, C.; Eds.; Springer Fachmedien: Wiesbaden, 2016; pp. 163−196.
(2) Carrara, L.; Giroud, C.; Concha-Lozano, N. Development of a Vaping Machine for the Sampling of THC and CBD Aerosols Generated by Two Portable Dry Herb Cannabis Vaporisers. *Med. Cannabis Cannabinoids* **2020**, *3* (1), 84−94.
(3) Munger, K. R.; Anreise, K. M.; Strongin, R. M. Cannabis Concentrate Vaping Chemistry. *Front. Toxicol.* **2025**, *7*, 1568207.
(4) Oswald, I. W. H.; Ojeda, M. A.; Pobanz, R. J.; Koby, K. A.; Buchanan, A. J.; Del Rosso, J.; Guzman, M. A.; Martin, T. J. Identification of a New Family of Prenylated Volatile Sulfur Compounds in Cannabis Revealed by Comprehensive Two-Dimensional Gas Chromatography. *ACS Omega* **2021**, *6* (47), 31667−31676.
(5) Oswald, I. W. H.; Paryani, T. R.; Sosa, M. E.; Ojeda, M. A.; Altenbernd, M. R.; Grandy, J. J.; Shafer, N. S.; Ngo, K.; Peat, J. R. I.; Melshenker, B. G.; Skelly, I.; Koby, K. A.; Page, M. F. Z.; Martin, T. J. Minor, Nonterpenoid Volatile Compounds Drive the Aroma Differences of Exotic Cannabis. *ACS Omega* **2023**, *8* (42), 39203−39216.
(6) Paryani, T. R.; Sosa, M. E.; Page, M. F. Z.; Martin, T. J.; Hearvy, M. V.; Ojeda, M. A.; Koby, K. A.; Grandy, J. J.; Melshenker, B. G.; Skelly, I.; Oswald, I. W. H. Nonterpenoid Chemical Diversity of Cannabis Phenotypes Predicts Differentiated Aroma Characteristics. *ACS Omega* **2024**, *9* (26), 28806−28815.
(7) Valizadehderakhshan, M.; Shahbazi, A.; Kazem-Rostami, M.; Todd, M. S.; Bhowmik, A.; Wang, L. Extraction of Cannabinoids from Cannabis Sativa L. (Hemp)—Review. *Agriculture* **2021**, *11* (5), 384.
(8) Pulido Bonilla, L. G.; King, J. W.; Gil Chaves, I. D. Comprehensive Review of Cannabis Processing Stages: A Comparison of Techniques for Obtaining High-Quality Extracts. *J. Appl. Res. Med. Aromat. Plants* **2025**, *49*, 100678.
(9) Lazarjani, M. P.; Young, O.; Kebede, L.; Seyfoddin, A. Processing and Extraction Methods of Medicinal Cannabis: A Narrative Review. *J. Cannabis Res.* **2021**, *3* (1), 32.
(10) López-Olmos, C.; García-Valverde, M. T.; Hidalgo, J.; Ferrerio-Vera, C.; Sánchez de Medina, V. Comprehensive Comparison of Industrial Cannabinoid Extraction Techniques: Evaluation of the Most Relevant Patents and Studies at Pilot Scale. *Front. Nat. Prod.* **2022**, *1*, 1043147.
(11) de Aguiar, A. C.; Vardanega, R.; Viganó, J.; Silva, E. K. Supercritical Carbon Dioxide Technology for Recovering Valuable Phytochemicals from Cannabis Sativa L. and Valorization of Its Biomass for Food Applications. *Molecules* **2023**, *28* (9), 3849.
(12) Boumghar, H.; Sarrazin, M.; Banquy, X.; Boffito, D. C.; Patience, G. S.; Boumghar, Y. Optimization of Supercritical Carbon Dioxide Fluid Extraction of Medicinal Cannabis from Quebec. *Processes* **2023**, *11* (7), 1953.
(13) Ribeiro Grijó, D.; Vieitez Osorio, I. A.; Cardozo-Filho, L. Supercritical Extraction Strategies Using CO2 and Ethanol to Obtain Cannabinoid Compounds from *Cannabis* Hybrid Flowers. *J. CO2 Util.* **2019**, *30*, 241−248.
(14) Fiorito, S.; Epifano, F.; Palumbo, L.; Collevecchio, C.; Genovese, S. A Subcritical Butane-Based Extraction of Non-Psychoactive Cannabinoids from Hemp Inflorescences. *Ind. Crops Prod.* **2022**, *183*, 114955.
(15) Duminy, J.-H.; Goosen, N.; Pott, R.; van Rensburg, E. Development of a Solvent Screening Methodology for Cannabinoid Recovery from a Wax By-Product via Recrystallization. *Biomass Convers. Bioref.* **2024**, *14* (16), 18637−18647.
(16) Duminy, J.-H.; Goosen, N.; van Rensburg, E.; Arries, W.; Mokwena, L.; Kotobe, L.; Pott, R. Application of Different Chromatographic Techniques to Characterise Wax By-Products Generated during Cannabinoid Extraction. *Biomass Convers. Bioref.* **2024**, *14* (16), 18923−18936.
(17) Leyva-Gutierrez, F. M. A.; Munafo, J. P., Jr.; Wang, T. Characterization of By-Products from Commercial Cannabidiol Production. *J. Agric. Food Chem.* **2020**, *68* (29), 7648−7659.
(18) De Poli, M.; Chenet, T.; Felletti, S.; Spadafora, D.; Cavazzini, A.; Franchina, F. A. Sorbent-Based Sampling With Two-Stage Trapping/Desorption Coupled to Comprehensive Two-Dimensional Gas Chromatography and Mass Spectrometry for Terpenoids Profiling in Cannabis. *Anal Sci. Adv.* **2025**, *6* (1), No. e202400044.
(19) Franchina, F. A.; Dubois, L. M.; Focant, J.-F. In-Depth Cannabis Multiclass Metabolite Profiling Using Sorptive Extraction and Multidimensional Gas Chromatography with Low- and High-Resolution Mass Spectrometry. *Anal. Chem.* **2020**, *92* (15), 10512−10520.
(20) Bush, R. T.; McInerney, F. A. Leaf Wax *n*-Alkane Distributions in and across Modern Plants: Implications for Paleoecology and Chemotaxonomy. *Geochim. Cosmochim. Acta* **2013**, *117*, 161−179.
(21) Cerda-Peña, C.; Contreras, S. Characterization and Chemo-Taxonomic Evaluation of Plant Leaf Waxes (Long Chain *n*-Alkanoic Acids, *n*-Alkanes and *n*-Alkanols) as a Vegetation Biomarker from Species of the South American Temperate Forest (STF). *Ecol. Indic.* **2022**, *136*, 108675.
(22) Scognamiglio, M.; Baldino, L.; Reverchon, E. Fractional Separation and Characterization of Cuticular Waxes Extracted from Vegetable Matter Using Supercritical CO2. *Separations* **2022**, *9* (3), 80.
(23) Janta, P.; Vimolmangkang, S. Chemical Profiling and Clustering of Various Dried Cannabis Flowers Revealed by Volatilomics and Chemometric Processing. *J. Cannabis Res.* **2024**, *6* (1), 41.
(24) Resende, G. A. P.; Ferraz, S. M. M.; Bressan, L. P.; de Oliveira, I.; Nazario, T.; de Araujo, L. P.; Hantao, L. W. Comprehensive Two-Dimensional Gas Chromatography Analysis of Volatiles on e-Liquids and Aerosol Compounds Produced during the Heating Process. *J. Chromatogr. Open* **2025**, *8*, 100273.
(25) Pedrini, N.; Ortiz-Urquiza, A.; Huarte-Bonnet, C.; Zhang, S.; Keyhani, N. O. Targeting of Insect Epicuticular Lipids by the Entomopathogenic Fungus Beauveria Bassiana: Hydrocarbon Oxidation within the Context of a Host-Pathogen Interaction. *Front. Microbiol.* **2013**, *4*, 24.
(26) Li, J.; Li, K.; Li, H.; Wang, X.; Wang, W.; Wang, K.; Ge, M. Long-Chain Alkanes in the Atmosphere: A Review. *J. Environ. Sci. China* **2022**, *114*, 37−52.
(27) Duminy, J.-H.; Van Rensburg, E.; Pott, R.; Goosen, N. Solvent-Assisted Recrystallisation for the Recovery of Cannabinoids from *Cannabis* Extraction by-Products. *Ind. Crops Prod.* **2024**, *209*, 117981.

https://doi.org/10.1021/acsomega.5c13451
ACS Omega XXXX, XXX, XXX−XXX